



Semnan University

Mechanics of Advanced Composite Structures

journal homepage: <http://MACS.journals.semnan.ac.ir>

Crashworthy Behavior of Plain Weave Glass/Epoxy Composite Tubes Containing Different Extents of Overlap of Dropped Plies

S. Kureel , Murari V. 

Department of Applied Mechanics, Motilal Nehru National Institute of Technology Allahabad, Prayagraj, 211004, India

KEYWORDS

Composite tubes;
Energy absorbers;
Ply drops;
Dropped-off plies;
Specific energy absorption.

ABSTRACT

Fiber-reinforced composite tubes offer numerous advantages over traditional metal tubes, including lower weight, higher strength and stiffness, corrosion resistance, and fatigue resistance. These tubes have the potential to act as energy absorbers, making it crucial to understand the factors influencing their energy-absorbing characteristics. This study focuses on experimentally investigating the crashworthiness of woven glass/epoxy composite tubes by analyzing the effects of the inner diameter and the extent of overlapping dropped-off plies. Circular cross-sectional tubes with different diameters (20, 25, and 30mm) and varying extents of ply overlap (0, $\frac{1}{4}$, $\frac{1}{2}$, $\frac{3}{4}$, and 1 times the circumference) are subjected to impact loading and quasi-static compressive loading. The length-to-diameter ratio remains constant across all cases. The investigation examines the influence of the inner diameter and the extent of overlapping plies on parameters such as mean crushing force, energy absorption, specific energy absorption, crush force efficiency, and stroke efficiency, and compares the damage and failure mechanisms observed in different composite tube configurations. The results highlight that specimens with smaller diameters and a half overlap exhibit maximum crush load efficiency, contrary to specimens with larger diameters and full overlap. This study emphasizes the significance of considering the extent of overlapping and its geometry to tailor the energy absorption characteristics of composite tubes for specific applications.

1. Introduction

The utilization of composite materials has expanded a thousand-fold in recent decades. Composites are used in many different fields owing to their advantageous characteristics, their ability to offer a superior strength-to-weight ratio, higher energy absorption capabilities, strong fatigue resistance, corrosion resistance, and lower environmental impact [1-5]. A significant amount of effort has been made to discover energy-absorbing structures that are crashworthy [6]. Crashworthiness is described as the capacity of a vehicle to sustain collisions and its ability to safeguard occupants and passengers from severe or deadly injuries [7]. Particularly in the automotive industry, composite tubes have grown as permanent energy absorbers [8, 9].

Composite tubes have excellent energy absorption capacity due to their complex and multiple failure modes. This makes them ideal for use in automotive crashworthiness applications. The energy-absorption in these structures depends on a number of factors, including reinforcement, matrix material, layer orientation, stacking sequence, cross-sectional shape, and position of trigger [10].

Othman et al. [11] performed crash analysis tests to examine the crushing mechanism and failure pattern in foam-filled tubular structures containing different thicknesses. They estimated the effect of filler material on the crashworthy behavior of pultruded composite tubes and observed that the profiles with and without foam filling have failed through fiber splaying and matrix crushing. Unidirectional composite tubes

* Corresponding author. Tel.: +91-9455388670
E-mail address: vmurari@mnnit.ac.in

reinforced with carbon fiber but with varying fiber orientations and wall thicknesses were studied by Wang et al. [12] for their energy absorption rate and crushing mode. They found that the tubes deform via brittle fracture failure mode generate less debris in impact loading than in quasi-static loading. Tube specimens were divided into two groups: one with the same wall thickness (3mm) but containing different fiber orientations ($\phi=15^\circ, 60^\circ$ & 75°) and the other with the same fiber orientation (45°) but with different thicknesses (2mm, 3mm, 4mm, 5mm, and 6mm). The study revealed that certain parameters related to crashworthiness (including mean crushing load, peak load, and energy absorbed) decreased in the first group, while only peak and mean load exhibited a linear increase in the other group, as thickness changed. Zhang et al. [13] examined the effect of thickness on the quasi-static crushing response of square aluminium tubes. The study revealed that in order to achieve an increase of 35% in energy absorption, the thickness of the corner of a square tube needed to be greater than that of its sides, while the maximum load capacity remained unchanged. Thornton et al. [14] inspected the effect of different types of constituent materials on the quasi-static crushing response of composite tubes. It was observed from the study that the specific energy absorption for different thermosetting matrices were found to be decreasing in the following order: epoxy, polyester, and phenolic. The specimens with 0° fiber orientation were found to possess a higher SEA in the case of glass fiber reinforced polymer (GFRP) tubes, where one or two outside 90° layers bind the 0° inner layer. In terms of section geometry, the SEA was found to be decreasing in the following order: round, square, and rectangular. Farley et al. [15] tested several composite specimen geometries consisting of carbon and kevlar as reinforcements to determine the energy absorption capability under constant rate crushing. It was concluded that as the ratio of diameter and thickness decreases, the SEA decreases as well. It was found that the specimens were geometrically scalable by varying the diameter and the wall thickness of the specimen at appropriate places in the case of kevlar/epoxy tubes. The same is not true in the case of tubes with carbon reinforcement. Patel et al. [16] examined the impact of several design variables on crush force dissipation parameters in automobile accidents. The peak load and the deformed length were used as crashworthiness parameters when testing a composite tube under axial and oblique compressive loads. Tube arrangement and fiber orientation of ply were influencing the crashworthiness parameter

during impact loading. It was found that GFRP material outperformed CFRP (carbon fiber reinforced polymer) material for oblique impact loads. In their research, Song et al. [17] investigated the response of metal-wrapped GFRP tubes under quasi-static compressive and impact loading. The failure mode is found to be influenced by factors such as the loading rate, wall thickness, and fiber orientation, which ultimately determine whether the tube would undergo stable crushing or catastrophic failure. The crushing behavior of laminated shells of different thicknesses in a cone form under axial compression was investigated by Kazemi et al. [18]. The buckling load was found to increase initially but subsequently reduced with an increase in the fiber orientation. Further, it was found that increasing the cone's original thickness has raised the buckling load. Turner et al. [19] examined two different thermoset matrix-based composite materials: a non-crimp fabric (NCF) and a continuous filament mat (CoFRM) with fiber volume fractions of 22% and 38%. The amount of binder has a considerable impact on the fracture toughness of mode I, while the composite tube's SEA seems to be quite forgiving of binder levels. Both materials' SEA levels seem to be tolerant to high void levels, opening the door to significant cost savings through expedited processing. Abosbaia et al. [20] investigated load-carrying capacity and energy absorption for segmented carbon and cotton fibers. Conversely, it was discovered that segmented composite tubes, incorporating tissue mat glass fibers, had a catastrophic failure mechanism and absorbed limited energy. Melo et al. [21] compared the effect of vacuum and non-vacuum production environments of composite tubes on the crushing behavior. The results show that crashworthy properties of polymer-based composite structures were highly influenced by controlled manufacturing processes. The crashworthy parameter was studied by Yan et al. [22] for tubes made of flax/epoxy reinforced composites with three different length-to-diameter (L/D) ratios, three different inner diameters (36, 54, and 82mm), and three different three-ply configurations (single, double, and triple) under quasi-static in-plane compressive loading. Additionally, it was discovered that a 36mm diameter tube with an L/d ratio of 2 and consisting of 3 layers achieved optimum SEA and crush load efficiency (CLE), which is superior to conventional metal tubes and almost as effective as GFRP and CFRP. Under quasi-static compression and drop weight impact, Gupta et al. [23] studied the crushing behavior and energy-absorbing capability of a glass/polyester hemispherical shell of varying thicknesses. As the thickness of the

hemispherical shell increases, the average crushing load also increases. Karbhari et al. [24] examined the post-crush response of biaxially and triaxially braided composite tubes made of three different types of fiber (glass, carbon, kevlar). They found that braiding changes the damage mechanism from stable crushing to lateral cracking when specimens were subjected to impact loading prior to quasi-static compression. Another study was reported by Tong et al. [25] on braided carbon/epoxy composite tubes for crash energy absorption. A novel chamfer trigger was developed and investigated under axial compressive loading. Further, it was found that cavities caused by chamfer lead in energy absorption up to 53% when the diameter-to-thickness (D/t) ratio increases. In this context, Farley et al. [26] categorized different crushing behavior of GFRP composite tubes subjected to different crushing speeds. They found that crushing behavior depends on crushing speed, constituent properties, and specimen geometry. The crushing mechanism for both (circular and square) GFRP composites was investigated by Palanivelu et al. [27] under several impact velocities showing a range from 9.3 to 14 meters per second. It is observed that circular tubes with a thickness of around 6% of their diameter exhibit 59% higher energy absorption capacity than the square tubes having a thickness of around 7.5% of their side length. According to Mahdi et al. [28], an optimized fiber orientation was created for GFRP composite tubes under in-plane quasi-static crushing. Tubes having circular cross-sections were prepared using epoxy-impregnated woven glass fiber fabric having different orientations. Further, they suggested that the ideal orientation of layers for stable crushing are $0^\circ/90^\circ$ and $+45^\circ/-45^\circ$, and the same for higher energy absorption is $+15^\circ/-75^\circ$ and that for both higher energy absorption and stable crushing is $+75^\circ/-15^\circ$. Liu et al. [29] investigated energy absorption in carbon/epoxy composite tubes using quasi-static and dynamic tests. It is found that strain rate significantly influenced crushing behavior, reducing crush load, and resulting in lower SEA values. Thicker tubes with $0^\circ/90^\circ$ layup and fabric architecture showed superior SEA performance. Diniz et al. [30] examined composite tubes made of different materials with drop-offs. It was found that carbon/aramid fabric had higher longitudinal elasticity modulus than carbon and glass. Carbon fabric tubes had the highest compression load capacity followed by hybrid tubular structures with four plies dropped. Khan & Mahdi [31] examined the effect of trigger mechanisms on glass epoxy/PVC hybrid composite tubes under axial compression. It is found that integrated trigger mechanisms

positively affect the crushing behavior and non-trigger specimens showed catastrophic failure modes. The double-step trigger outperformed the chamfer trigger in load-bearing capacity, energy absorption capacity, and crush force efficiency. Chen et al. [32] studied axial crushing response and crashworthiness characteristics of circular carbon/epoxy composite tubes. CFRP tubes achieved the best crashworthiness performance with a Specific Energy Absorption of 78.8 kJ/kg and a Maximum Crushing load of 485.7 kN. Also, it is found that fiber hybridization mainly affects post-crash integrity and crashworthiness characteristics, with negligible influence on crushing failure mode.

Many studies have examined the crashworthiness parameters of composite tubes. Improving crashworthiness in composite tubes holds the potential for various benefits, including enhanced occupant protection, reduced risk of injuries, and increased structural integrity during collisions. Composite materials provide engineers with the opportunity to tailor their properties to specific crash scenarios, allowing for optimized energy absorption, deformation mitigation, and enhanced crash resilience. By investigating factors such as material composition, fiber orientation, layup configuration, and geometrical parameters, researchers can further advance the understanding and practical application of composite materials in crashworthiness. The goal is to improve safety measures and protect human lives in critical impact situations. To this end, the present work focuses on the effect of geometry parameters on the crashworthiness of composite tubes. Comprehending the compressive behavior of composite tubes with the extent of overlap of dropped-off plies is an area that still needs investigation. To effectively estimate the crashworthiness, understanding the impact of the extent of overlap between dropped-off layers on crashworthiness parameters is crucial. The present research examines the consequences of the extent of overlap and inner diameter on the damage response and the crashworthiness parameters of composite tubular specimens subjected to quasi-static compression and those subjected to impact loading.

2. Methodology

2.1. Specimen Geometry/Boundary Conditions

To better understand how the extent of overlap affects crushing response, test specimens featuring the basic geometrical characteristics as shown in Figure 1 are analyzed. Throughout the study, the extent of overlapping remained constant along the length of the specimen. In this study, composite tubes with three different inner

diameters (20, 25, and 30mm) are considered. The lengths of the composite tubes are fixed so that the L/D ratio turns out to be 2.5.

The different extents of overlaps in each case are defined as the fraction of the circumference of the composite tube. Five different extents of overlap are taken into account: 0, 1/4, 1/2, 3/4, and 1 times the circumference of the composite tube. Pictorial representations of different extents of overlap are presented in Figure 2 showing the cross-sections of the specimens.

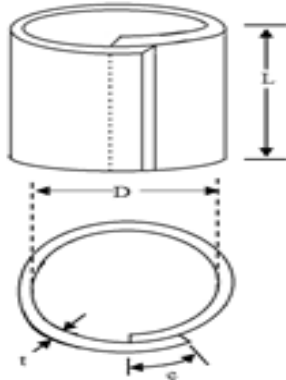


Fig. 1. Basic geometrical feature of test specimen (L, D, t, e are length, inner diameter, thickness and extents of overlap respectively)

Three different inner diameters each with five different extents of overlap make fifteen numbers

of cases in total. Four test specimens per case are prepared for performing the quasi-static compression test and three test specimens per case are prepared for performing the impact tests. The details of the different cases considered are presented in Table 1. The specimen codes mentioned in the table are to be interpreted as follows. For example, the first three letters 'WCT' in code 'WCT20_NO' stands for Woven Composite Tube, the next two digits represent the inner diameter of the specimen, the characters/number following the underscore symbol represents the extent of overlap. Here 'NO' indicates no overlap, '1.250' indicates 1/4 overlap, and so on.

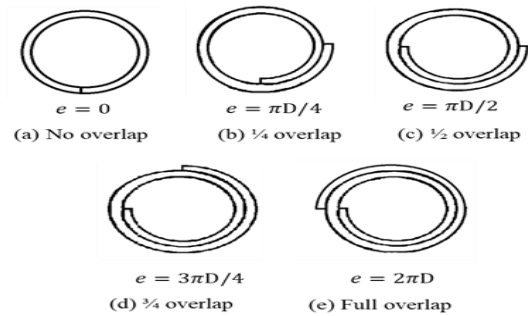


Fig. 2. Extent of overlap in different cases (D, inner diameter of the tube)

Table 1. Details of the specimens used in different cases

Case	Extent of Overlap	Diameter (mm)	Weight (gm)	Specimen Code	Average Thickness (mm)	Length (mm)
1	Zero Overlap	20	2.5	WCT20_NO	0.5	50
2		25	3.9	WCT25_NO	0.5	62.5
3		30	5	WCT30_NO	0.5	75
4	1/4 or Quarter Overlap	20	3.2	WCT20_1.250	0.6	50
5		25	4.6	WCT25_1.250	0.6	62.5
6		30	6.5	WCT30_1.250	0.6	75
7	1/2 or Half Overlap	20	3.8	WCT20_1.50	0.7	50
8		25	5.2	WCT25_1.50	0.7	62.5
9		30	8.6	WCT30_1.50	0.7	75
10	3/4 or Three-Quarter Overlap	20	4.5	WCT20_1.750	0.8	50
11		25	6.0	WCT25_1.750	0.8	62.5
12		30	9.0	WCT30_1.750	0.8	75
13	1 or Full Overlap	20	4.8	WCT20_2.0	1.0	50
14		25	7.2	WCT25_2.0	1.0	62.5
15		30	10.5	WCT30_2.0	1.0	75

During the manufacturing of the specimens, a plain weave woven E-glass 350 GSM fabric is utilized as reinforcement. The matrix is a combination of epoxy (LY556) and amine hardener (HY951) in a 10:1 ratio. All specimens are prepared using the hand lay-up method. Both the ends of the specimen were made flat and parallel to each other, no triggering features for damage initiation such as chamfering, etc. are provided in the specimens. Figure 3 displays photographs of the different specimens constructed for testing.



Fig. 3. Composite tubes with different inner diameters containing different extents of overlap

2.2. Experimental Setup

The specific details regarding the machine used for conducting the tests are as follows:

The in-plane quasi-static crushing is performed on a TINIUS OLSEN (L-series) machine. The machine has a piezo-based load cell of 10 kN and is designed to operate with an external personal computer installed with the software package to obtain the recorded data of the experiment. The videography of the specimen under crushing is done to analyze the failure mechanism. For each case, a group of four samples is subjected to testing. To execute the impact loading, the IMATEK IM10T-20HV drop weight impact test platform [33] is utilized. This equipment runs on the IMATEK IMPACT ANALYSIS software package. A data collection system equipped with a laser is employed to record approximately 4,000 data points within a 20-millisecond timeframe. In the case of quasi-static compression testing the bottom end of the tube is simply supported, while the compressive load is applied to the top end. In the case of drop weight impact testing, the weight is dropped from above to impact the top end of the specimen, with the bottom simply supported. The testing parameters used for impact loading are specified in Table 2. In each case, a total of three samples are tested.

Table 2. Impact test parameters

Impact mass (kg)	Striker mass (kg)	Striker Type	Impact energy (J)
36	7.75	Circular flat ($\phi=165$ mm)	20 to 200

3. Results and Discussions

The effect of inner diameter and the extent of overlapping of dropped-off plies on the parameters affecting the crashworthiness of composite tubes are discussed in the following subsections.

3.1. Effect of Extent of Overlap and Inner Diameter on the Response of Specimen Under Quasi-Static Crushing

In general, the entire crushing process during the quasi-static compression could be split into three different zones: preliminary crushing, crushing, and compaction (refer to Figure 4). During the preliminary crushing stage, the specimens were found to exhibit a linear load-displacement response until peak load (P_{peak}) was attained. During the crushing stage, a gradual failure process is observed. The damage mostly begins at the top portion of the tubes and the damaged portions start bending inwards and outwards, followed by the damage at the bottom portion of the specimen. This is observed as an initial steep decrease in the load and a subsequent cyclic increase and decrease in the load. These observations correspond to the process of damage formation and the bending of the damaged portion of the crushed specimen at both the loading and the supporting end of the specimen. The crush load has remained almost constant with slight fluctuations around P_{mean} . Finally, in the compaction zone, debris that got filled inside of the remaining tube densifies, and that results in a sudden rise in load.

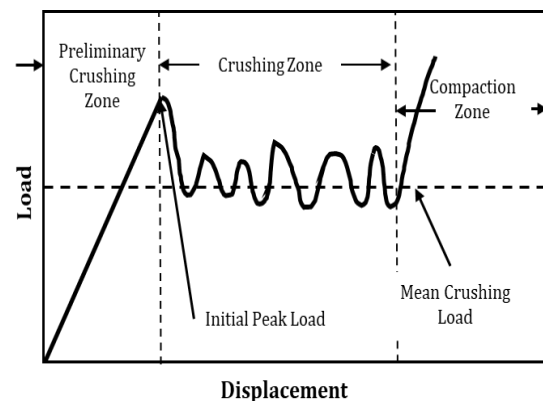


Fig. 4. Typical response of a composite tube specimen subjected to quasi-static crushing

The mechanical response of the specimens with different inner diameters containing no overlap is presented in Figure 5 and the same for other cases of overlaps are shown in Figures 6 to 9 respectively. The effect of different extents of overlap of dropped-off plies (such as no overlap, quarter, half, three quarter, and full overlap) on the mechanical response of the test specimen with 20mm inner diameter is presented in Figure

10 and that for the case with other diameters (25 and 30mm) are presented in Figure 11 and 12 respectively. It can be seen from Figure 5 to Figure 9 that the influence of the inner diameter diminishes as the amount of overlap grows. Further, it is observed that the crushing of specimens becomes more uniform with the increasing extent of overlap. From Figure 10 to Figure 12, it is observed, for all the cases of inner diameter considered, that the value of peak load increases around four times with an increase in the extent of overlap from no overlap to full overlap. In addition, it has been shown that an increase in the P_{peak} and P_{mean} occurs when the inner diameter of the specimen is increased.

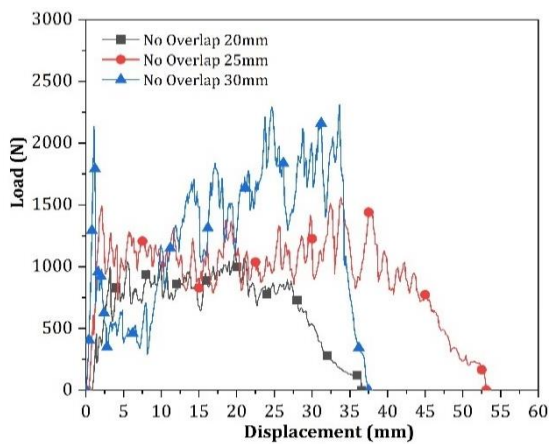


Fig. 5. Response of specimens with different inner diameters containing no overlap under quasi-static crushing

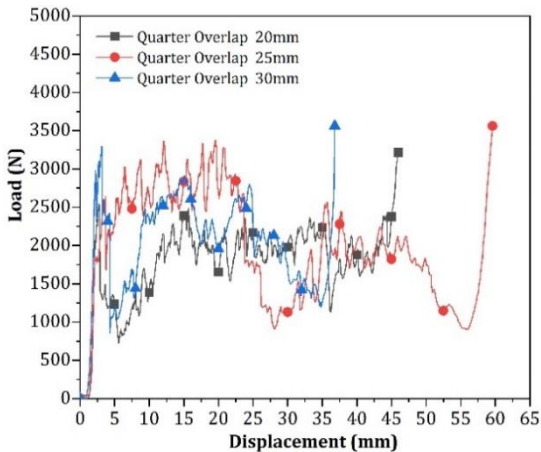


Fig. 6. Response of specimens with different inner diameters containing quarter overlap under quasi-static crushing

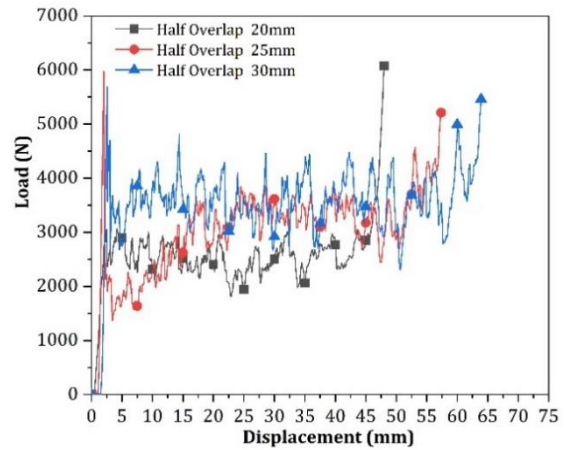


Fig. 7. Response of specimens with different inner diameters containing half overlap under quasi-static crushing

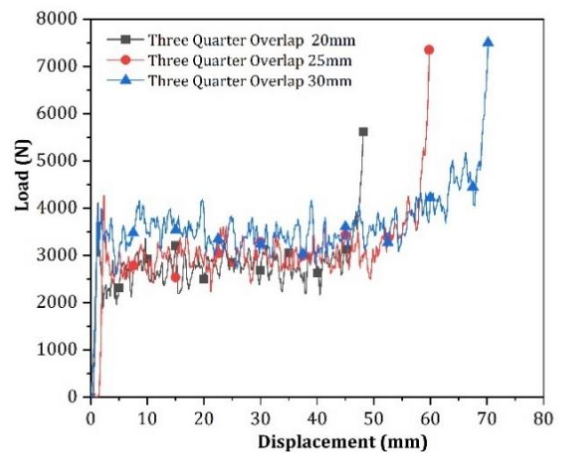


Fig. 8. Response of specimens with different inner diameters containing three-quarter overlap under quasi-static crushing

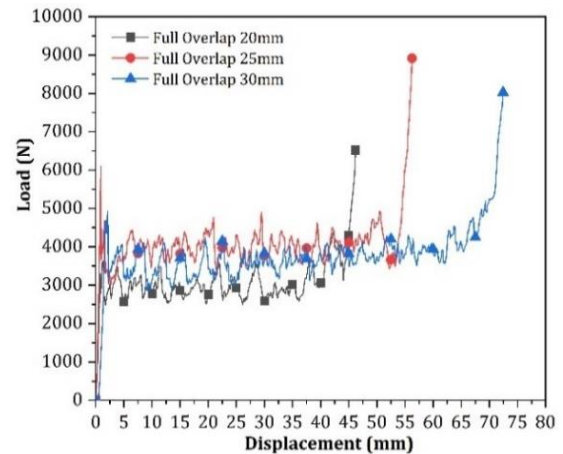


Fig. 9. Response of specimens with different inner diameters containing full overlap under quasi-static crushing

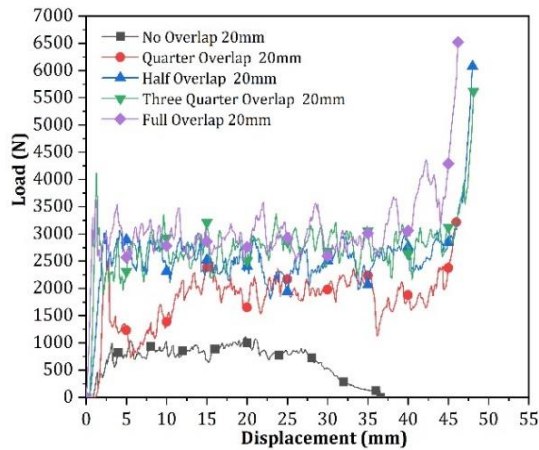


Fig. 10. Response of specimens with 20mm inner diameter with different extents of overlap: quasi-static crushing

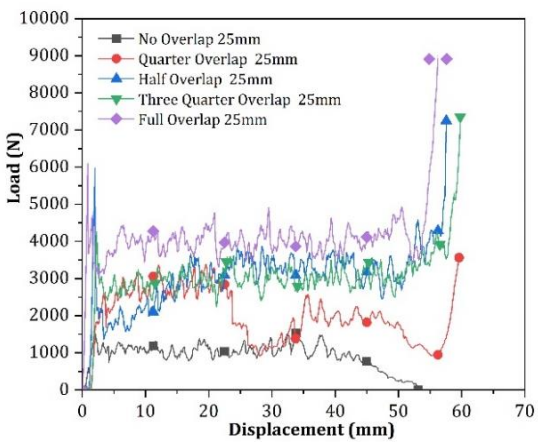


Fig. 11. Response of specimens with 25mm inner diameter with different extents of overlap: quasi-static crushing

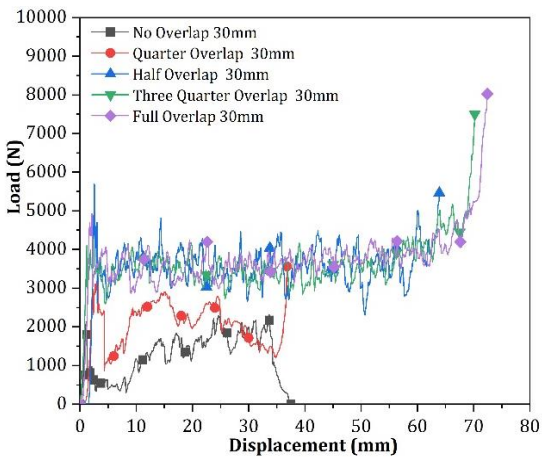


Fig. 12. Response of specimens with 30 mm inner diameter with different extents of overlap: quasi-static crushing

3.1.1. Energy Absorption (EA)

The amount of energy absorption is determined from the region underneath the load-displacement curve in the crushing zone. Figure 13 shows the amount of energy absorbed by test specimens, with different inner diameters and different extents overlap, under quasi-static compressive loading. After conducting tests on

different specimens, it has been found that the total amount of energy absorbed ranges from 20J to 250J, depending on the specific case. An increase in the amount of absorption of energy is noted when there is an increase in both inner diameter and the extent of overlap in the samples. However, for a set of test specimens with a particular diameter, the amount of energy absorption for an increase in the extent of overlap from no overlap to half overlap is smaller than that for an increase in the extent of overlap from half overlap to full overlap.

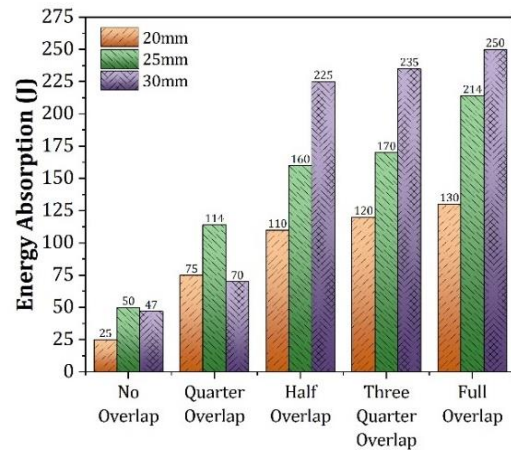


Fig. 13. Energy absorption in specimen with different extents of overlap and inner diameter: quasi-static crushing

The study indicates that the geometry of the overlap has a strong influence on the ability of the specimen to absorb energy. Specifically, it has been observed that samples with larger inner diameters, containing larger extents of overlap, have a higher capacity for energy absorption compared to those with smaller inner diameters and smaller extents of overlap.

3.1.2. Specific Energy Absorption (SEA)

Specific energy absorption (SEA) is calculated by dividing the amount of energy absorption in a specimen by its crushed mass. The SEA is a useful measure for assessing the energy absorption capabilities of specimens that have different inner diameters and different extents of overlap. From Figure 14, it is observed that the SEA for all the cases of inner diameters increases as the extent of overlap increases from no overlap to half overlap. With further increase in the extent of overlap from half overlap to full overlap, a decrease in the SEA is observed for the composite tube with 30mm diameter and only a little change is observed in the case of the composite tube with other smaller diameters. The SEA of tubes with larger diameters are found to be smaller than that of the tubes with smaller diameter. This is observed in all the cases of extents of overlap, except the case with no overlap. These

observations suggest that the appropriate choice of extents of overlap and inner diameter will result in a tailored crushing response.

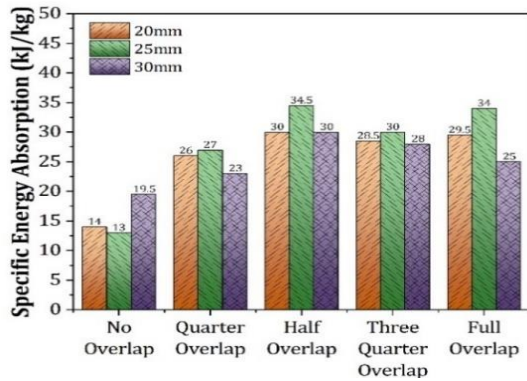


Fig. 14. Specific energy absorption in specimen with different extents of overlap and inner diameter: quasi-static crushing

3.1.3. Mean Crushing Load (P_{mean})

The “mean crushing load” (P_{mean}) is the average load in the crushing zone of the load-displacement curve.

The mean crushing load of test specimens with different inner diameters and different extents of overlap are shown in Figure 15. The results show that for smaller inner diameters (20mm and 25mm), P_{mean} increases as the extent of overlap increases. This can be attributed to the larger contact area and improved load distribution within the crushing zone as the extent of overlap grows. The increased overlap results in a greater load-bearing area, leading to enhanced load-carrying capacity and higher mean crushing load values. However, for the larger inner diameter (30mm), the P_{mean} increases when the extent of overlap increases from no overlap to half overlap, and then remains constant for further increases in the extent of overlap. These observations suggest that the relationship between the extent of overlap and the mean crushing load differs based on the inner diameter of the composite tubes. Smaller inner diameters exhibit a continuous increase, while larger inner diameters reach a saturation point where the mean crushing load stabilizes after a certain extent of overlap.

3.1.4. Crush Load Efficiency (CLE)

Crush load efficiency (CLE) is the amount of crushing load that is effectively prevented from getting transmitted from the loading end to the other end of the energy absorber. It is defined as the ratio of P_{mean} to P_{peak} . This measure is used in the crash safety sectors to determine the danger of head and neck injuries during a collision, and also to determine how much load is transferred to the operator or others during a crash. Figure 16 shows the effect of the extent of overlap and inner diameter on the crush load efficiency of test

specimens subjected to quasi-static crushing. The crush load efficiency of all the specimens is found to be above 60%, except in the case of specimens with 30mm diameter containing no overlap and the specimen with 25mm diameter containing half overlap. Further, it is found that the crush load efficiency of 30mm diameter composite specimens increases monotonically when the extent of overlap is increased from no overlap to full overlap, whereas the crush load efficiency of the composite tubes with 25mm diameter decreases initially with an increase in the extent of overlap from no overlap to half overlap and then increases with further increase in the extent of overlap to full overlap. In the case of composite tubes with 20mm diameter, an increase in crush load efficiency is noted initially when the extent of overlap is increased from no overlap to half overlap and then has reduced magnitudes with further increase in the extent of overlap to full overlap. In addition to this, crush load efficiency is seen to be at its highest when composite tubes have a 20mm diameter with half overlap. These findings imply that optimizing the inner diameter and the extent of overlap might boost the crush load efficiency of the composite tubes.

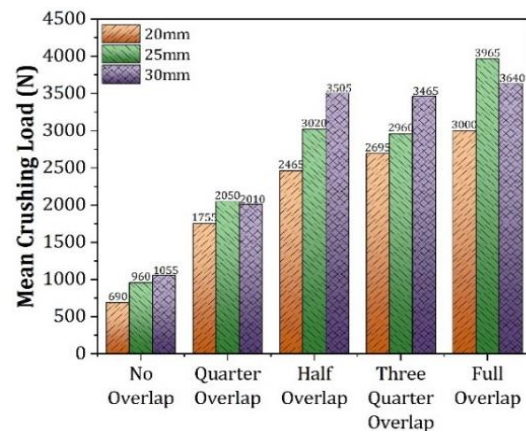


Fig. 15. Mean crushing load in specimen with different extents of overlap and inner diameter: quasi-static crushing

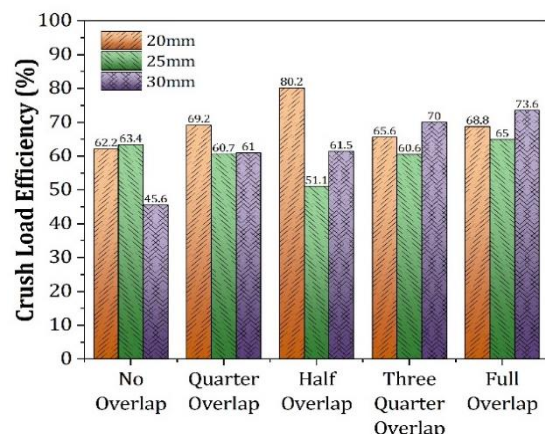


Fig. 16. Crush load efficiency in specimen with different extents of overlap and inner diameter: quasi-static crushing

3.2. Effect of Extent of Overlap and Inner Diameter on the Crushing Response of Specimens Under Impact Load

This section discusses the impact loading response of composite tubes with varying inner diameters and extents of overlap. To prevent post-crushing compaction of the test specimens, a specific amount of impact energy (IE) is carefully selected. The results of the impact testing for different test specimen scenarios are compiled in Table 3, which presents various crashworthiness parameters. The effect of inner diameter on the load-displacement responses of the test specimens having different extents of overlap subjected to impact loading are presented in Figure 17 to Figure 21, and the effect of extent of overlap on the load-displacement responses of specimens with different inner diameter subjected to impact loading are presented in Figure 22 to Figure 24. Further, in the case of tubes with 25mm diameter containing quarter, half, and full overlap (refer Figure 23), a gradual increase in the load levels with progressive damage and crushing is observed. This reduced initial peak load and gradually increasing load levels with progressive damage is a desired characteristic for an improved crashworthiness behavior. A similar response is observed in the case of quasi-static compression, for the specimen having a 25 mm diameter containing a quarter overlap (refer to Figure 6).

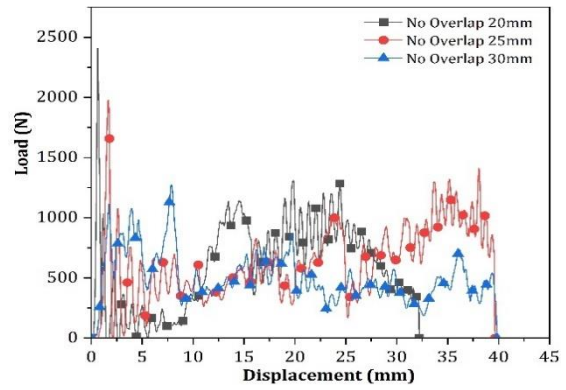


Fig. 17. Response of specimens with different inner diameters containing no overlap: crushing under impact load

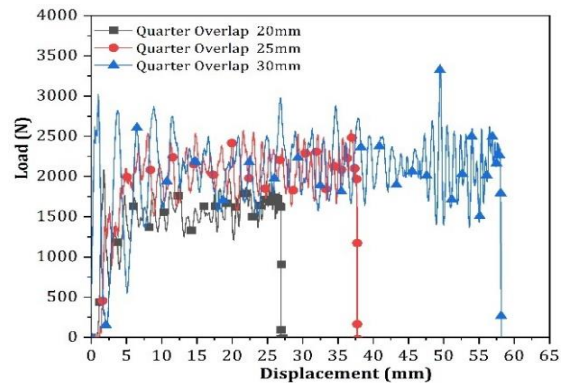


Fig. 18. Response of specimens with different inner diameters containing quarter overlap: crushing under impact load

Table 3. Crashworthiness parameter

Extent of overlap	ID (mm)	Crushed mass (gm)	CL ¹ (mm)	IE ² (J)	EA ³ (J)	P _{peak} (N)	P _{mean} (N)	η _{stroke} (%)	CFE ⁴ (%)	SEA ⁵ (kJ/kg)
Zero Overlap	20	1.59	32	20	18	2410	625	64	26	11.3
	25	2.5	40	25	25	1980	665	64	33.5	10
	30	2.66	40	20	20	1275	490	53.4	38.5	7.5
¼ or Quarter Overlap	20	1.73	27	30	30	2090	1195	54	57.3	17.3
	25	2.76	37.5	75	73	2585	1840	60	71	26.5
	30	5.02	58	120	120	3390	2065	77.4	60.8	24
½ or Half Overlap	20	1.3	17.5	40	36	4620	1895	35	41.1	27.7
	25	2.41	29	70	69	3365	2345	46.5	69.6	28.6
	30	4.58	40	115	115	4320	3050	53.4	70.6	25.1
¾ or Three-Quarter Overlap	20	1.8	20	60	57	4840	2620	40	54.2	31.7
	25	3.45	36	115	112	5545	2900	57.6	52.3	32.5
	30	3.42	28.5	115	110	8509	4225	38	49.6	32.2
1 or Full Overlap	20	2.87	30	70	70	3020	2160	60	71.5	24.4
	25	3.6	31.5	115	112	4865	3575	50.4	73.5	31.2
	30	5.86	42	170	165	6345	4045	56	63.7	28.1

¹ CL= crushed length

² IE= impact energy

³ EA= energy absorb

⁴ CFE= crush force efficiency

⁵ SEA= specific energy absorption

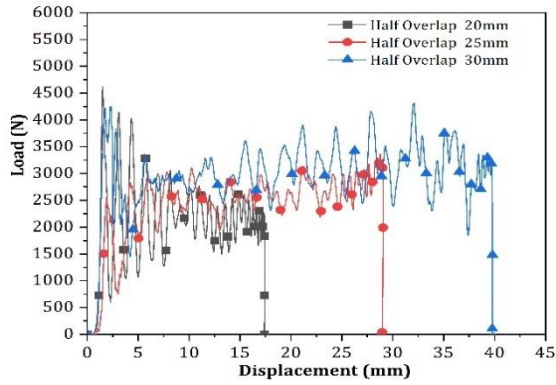


Fig. 19. Response of specimens with different inner diameters containing half overlap: crushing under impact load

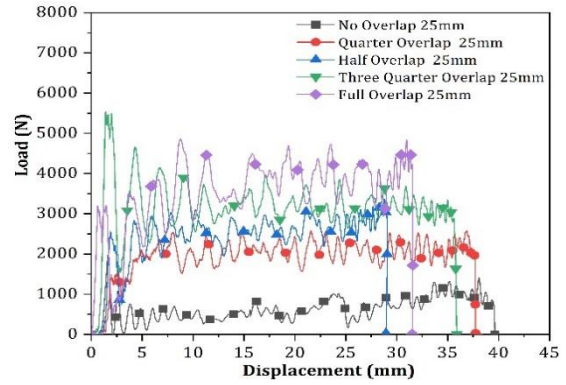


Fig. 23. Response of specimens with 25mm inner diameter with different extents of overlap: crushing under impact load

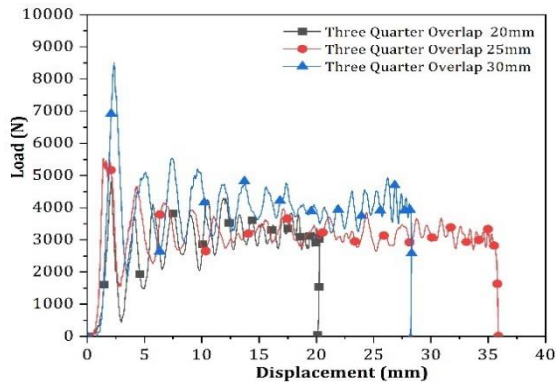


Fig. 20. Response of specimens with different inner diameters containing three-quarter overlap: crushing under impact load

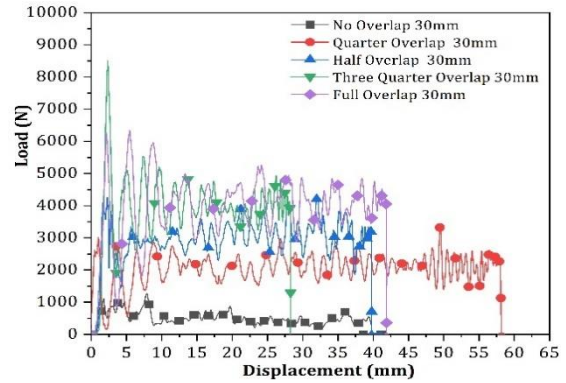


Fig. 24. Response of specimens with 30mm inner diameter with different extents of overlap: crushing under impact load

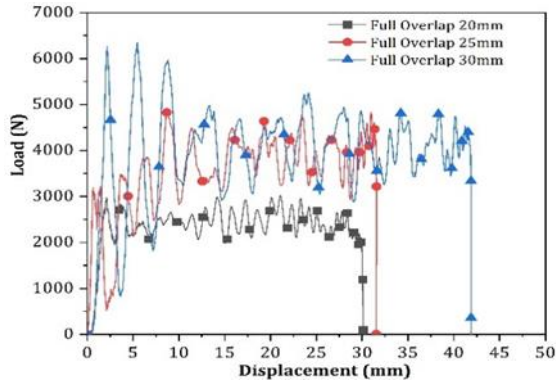


Fig. 21. Response of specimens with different inner diameters containing full overlap: crushing under impact load

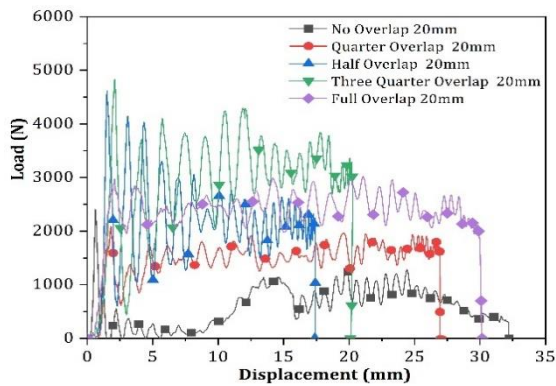


Fig. 22. Response of specimens with 20mm inner diameter with different extents of overlap: crushing under impact load

3.2.1. Energy Absorption (EA)

Energy absorption in the test specimens with different extents of overlap and different inner diameters subjected to impact loading are presented in Figure 25. An increase in the absorption of energy is noted when the inner diameter and the extent of overlap in the specimen are increased. However, the effect of extent of overlap on energy absorption is more significant than the effect of inner diameter.

3.2.2. Specific Energy Absorption (SEA)

Figure 26 shows the effect of the different extents of overlap and different inner diameters on the energy absorbed per unit mass of crushed composite tubes under dynamic crushing. The specific energy absorption (SEA) for various test specimens ranges from 7.5 kJ/kg to 32.5 kJ/kg. An increase in the value of SEA is noted when the extent of overlap increases from no overlap to half overlap and thereafter differences in SEA are less. Additionally, composite tubes with larger inner diameters have lower SEA compared to those with smaller inner diameters, which is consistent with the observation from quasi-static loading (see Figure 14). It is worth noting that, except for cases with half overlap, the SEA for composite tubes subjected to impact loading is found to be more than the corresponding quasi-static cases.

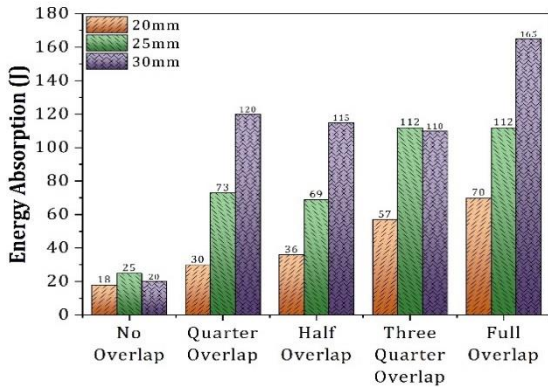


Fig. 25. Energy absorption in specimen with different extents of overlap and inner diameter: crushing under impact load

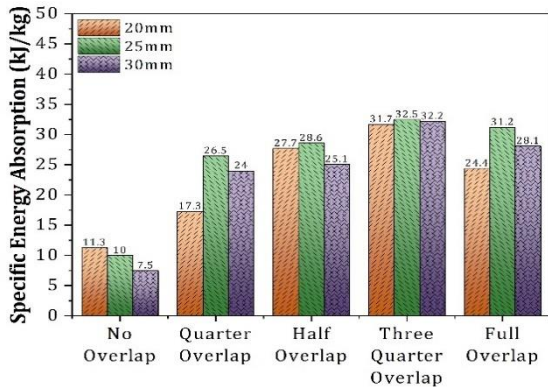


Fig. 26. Specific energy absorption in specimen with different extents of overlap and inner diameter: crushing under impact load

3.2.3. Mean Crushing Load (P_{mean})

Figure 27 shows the effect of different extent of overlap and different inner diameters on the mean crushing load (P_{mean}) of composite tubes subjected to crushing under impact load. The Figure reveals that, except for the case of no overlap, the mean crushing load increases with increasing diameter for all extents of overlap. In terms of loading instance, the mean crushing load for composite tubes subjected to impact loading is smaller than that obtained for quasi-static loading (refer Figure 15), except for the cases of composite tubes with 30 mm diameter containing quarter, three-quarter, and full overlap. The percentage increase in mean crushing load for different cases under impact load is around 2% to 21% as compared to quasi-static crushing. Notably, the mean crushing load is highest for the case of three-quarter overlap, rather than full overlap.

3.2.4. Crush Load Efficiency (CLE)

The effect of different extents of overlap and inner diameter of the test specimens subjected to impact load on the crush load efficiency (CLE) are shown in Figure 28. The crush load efficiency is found to be above 60% (refer Figure 28) for the

specimens with inner diameters of 25 mm and 30 mm that have quarter, half, or full overlap and for the specimens with inner diameter of 20mm containing full overlap. This observation is in contrast to that noted in the case of quasi-static loading (refer to Figure 16), where the crush force efficiency for almost all the cases were above 60%. When compared to the results obtained for the cases under quasi-static load, the crush force efficiency of the specimens with no overlap and those with three-quarter overlap under impact loading was found to be reduced by 60% and 30%, respectively. On the other hand, an increase in the crush force efficiency is noted in the case of specimens with 25 mm inner diameter containing quarter, half, and full overlap; specimens with 20mm diameter containing full overlap and specimens with 30mm diameter containing half overlap.

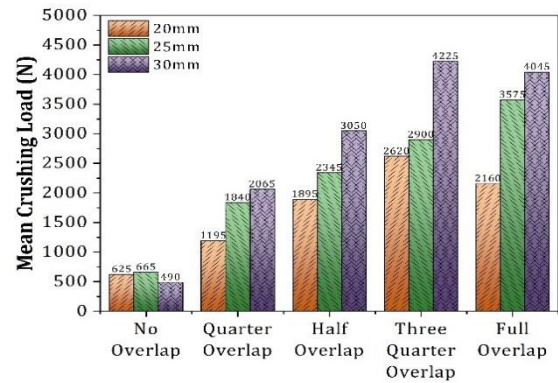


Fig. 27. Mean crushing load in specimen with different extents of overlap and inner diameter: crushing under impact load

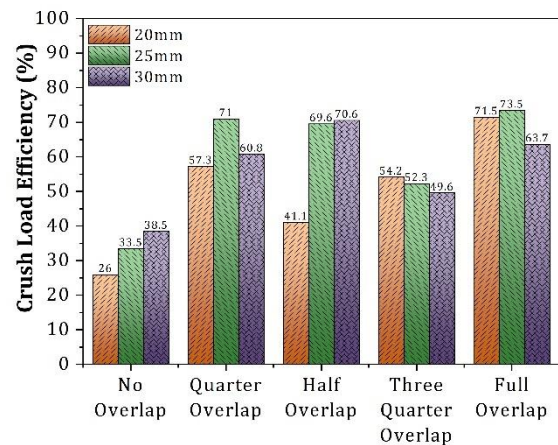


Fig. 28. Crush load efficiency in specimen with different extents of overlap and inner diameter: crushing under impact load

3.2.5. Stroke Efficiency (η_{stroke})

Stroke efficiency (η_{stroke}) is defined as the ratio of total crushable length to the total length of the specimens being considered. Figure 29 shows the effect of different extents of overlap and different inner diameters on the stroke efficiency of

composite tubes under dynamic crushing. The stroke efficiency (η_{stroke}) in most of the cases of composite tubes are found to be more than 50%, with a maximum value of 77.4% in the case of the composite tube with a 30mm diameter containing a quarter overlap. Stroke efficiency of less than 50% is found in the case of composite tubes containing half overlap (with 20mm and 25mm diameter) and those containing three-quarter overlap (with 20mm and 30 mm diameter).

3.3. Effect of Extent of Overlap and Inner Diameter on Crushing Behavior and Failure Mechanism

The crushing behavior of composite tubes with different inner diameters containing different extents of overlap at different instances during impact loading are presented in Figures 30 to 34. Typically, composite tubes with different inner diameters and different extents of overlap experience gradual crushing, along with fibers on the exterior or interior splaying simultaneously. In the case of the composite tube with a 20 mm inner diameter containing no overlap (refer to Figure 30 (a)), the crushing is seen to be occurring at both ends of the specimen whereas in the case of 25 mm (refer to Figure 30 (b)) crushing is to be occurring only at the top end. In the case of the specimen with a 30 mm diameter containing no overlap, a circumferential crack is seen at the mid-span of the specimen (ref. fig. 30(c)).

The specimens with different inner diameters containing some amount of overlap show a steady progressive crushing at the loading end of the test specimen. Further, no mid-span cracking and no simultaneous crushing at both ends are seen in these cases.

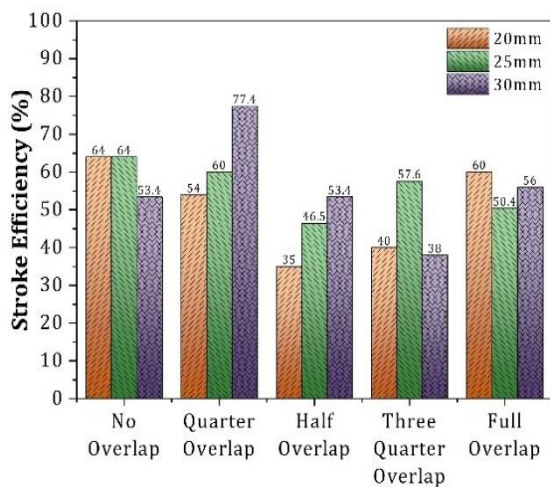


Fig. 29. Stroke efficiency in specimen with different extents of overlap and inner diameter: crushing under impact load

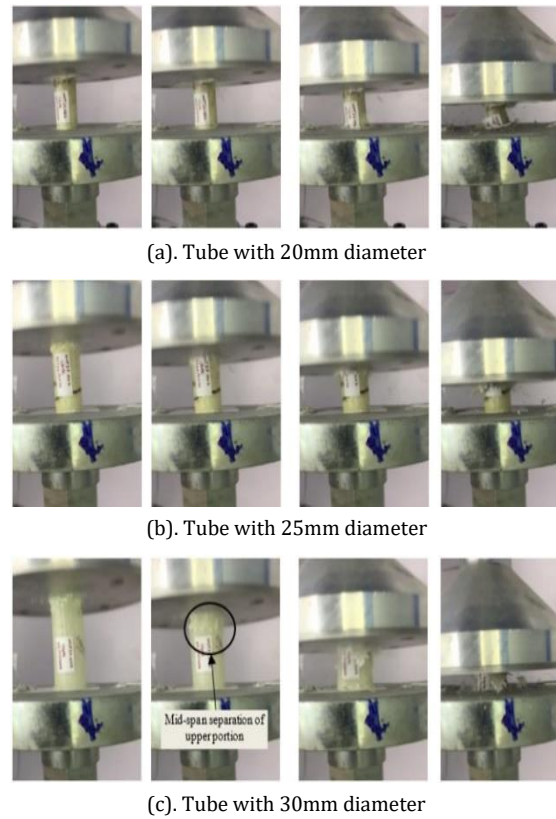


Fig. 30. Crushing behavior of composite tube with different diameters containing no overlap extent subjected to impact loading

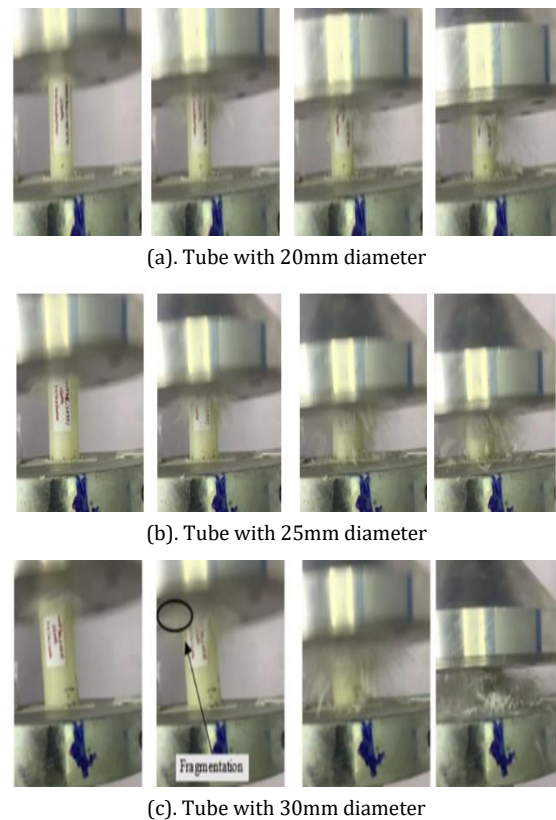
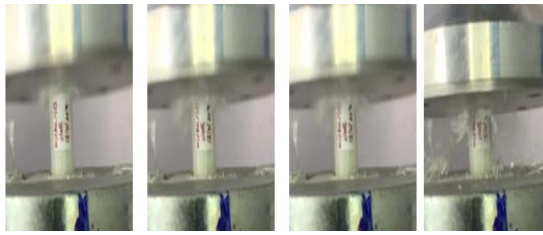


Fig. 31. Crushing behavior of composite tube with different diameters containing quarter overlap extent subjected to impact loading



(a). Tube with 20mm diameter

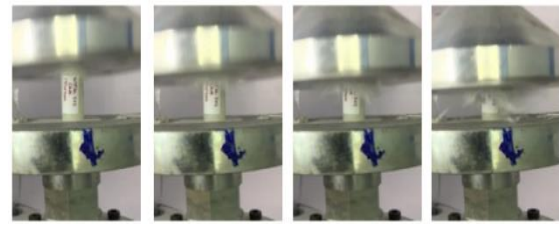


(b). Tube with 25mm diameter

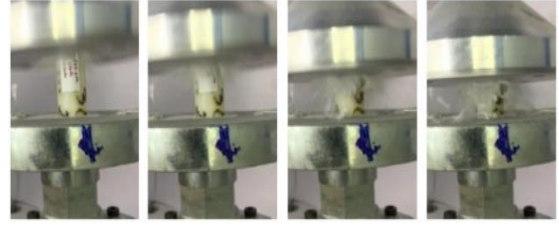


(c). Tube with 30mm diameter

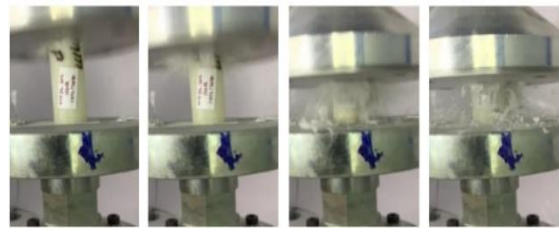
Fig. 32. Crushing behavior of composite tube with different diameters containing half overlap extent subjected to impact loading



(a). Tube with 20mm diameter

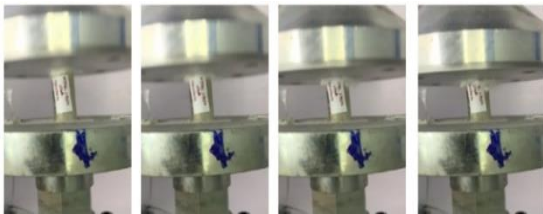


(b). Tube with 25mm diameter

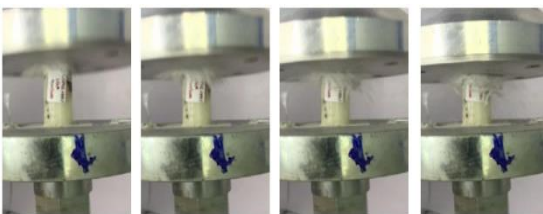


(c). Tube with 30mm diameter

Fig. 34. Crushing behavior of composite tube with different diameters containing full overlap extent subjected to impact loading



(a). Tube with 20mm diameter



(b). Tube with 25mm diameter



(c). Tube with 30mm diameter

Fig. 33. Crushing behavior of composite tube with different diameters containing three-quarter overlap extent subjected to impact loading

Figures 35 and 36 show the distinct types of failure that are observed in different cases of specimens subjected to quasi-static compression and impact loading respectively. The specimens with a smaller inner diameter and lesser extent of overlap subjected to impact loading fail through combined crushing at the end and delamination/kinking of the overlap portion (refer to Figure 35 (a) & (b)). Splaying fronds are developed up to some length and then they fail through collision with uncrushed portions in composite tubes containing no overlap and quarter overlap. Composite tubes containing larger extents of overlap (half, three-quarters, and full) fail through progressive crushing with petal formation and fiber splaying as shown in Figures 35 (c) & (d). In the case of composite tubes with smaller diameters containing no overlap and quarter overlap, subjected to quasi-static compression, cracks developed at the mid-span of the tube and then propagated around its circumference, as shown in Figures 36 (a) & (b). This resulted in an unstable crushing upon further loading. In the case of composite tubes containing half, three-quarters, and full overlap, progressive crushing that resulted in compaction as shown in Figures 36 (c) and (d) is observed.

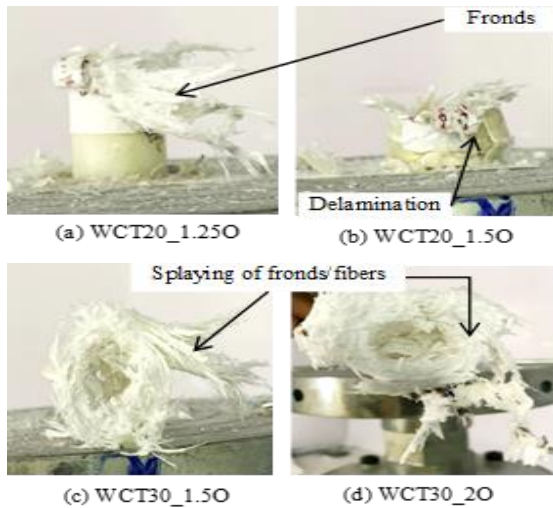


Fig. 35. Failure mechanism found in different specimens subjected to impact loading

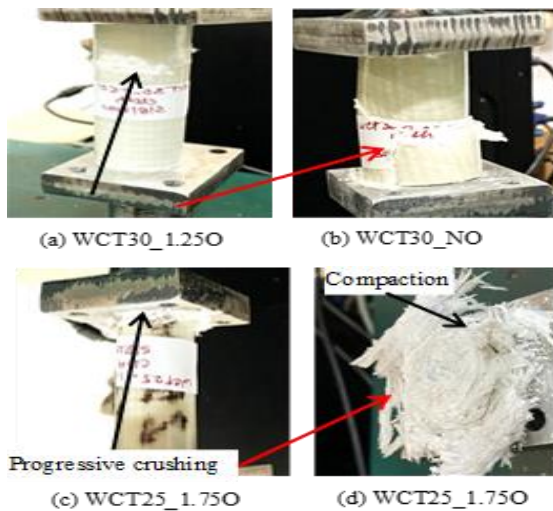


Fig. 36. Failure mechanism found in different specimens subjected to quasi-static crushing

4. Conclusions

The present study aims to systematically understand the influence of inner diameter and the extent of overlap of dropped-off plies on crashworthiness parameters of woven glass/epoxy composite tubes. To the best of the authors' knowledge, the needed focus has not been given in the literature to the study of the effect of the geometry of the overlaps resulting from ply drops on the crashworthiness of composite tubes. These features are found to influence the crushing behavior and thus can lead to a specific and tailor-made damage behavior, which is a desired factor in utilizing composite specimens for crash applications.

Composite tubes with three different diameters (20mm, 25mm, and 30mm) and various extents of overlap (0, $\frac{1}{4}$, $\frac{1}{2}$, $\frac{3}{4}$, 1 overlap) were considered in the study. Quasi-static compression and impact loading tests were conducted on the specimens. The following

results indicate that the inner diameter of the composite tubes and the extent of overlapping of dropped-off plies are crucial in achieving tailor-made crashworthiness characteristics.

1. Maximum crush load efficiency was observed in specimens with smaller diameters containing half overlap, while larger diameter specimens with full overlap showed lower efficiency.
2. Impact-loaded specimens exhibited higher crush load efficiency and specific energy absorption compared to specimens subjected to quasi-static crushing.
3. Specimens with different diameters and a three-quarter overlap demonstrated the highest specific energy absorption, while composite tubes with a 30mm diameter and a quarter overlap achieved maximum stroke efficiency.

Availability of Data

The datasets used or analyzed during the current study are available from the corresponding author upon reasonable request.

Conflicts of Interest

The author declares that there is no conflict of interest regarding the publication of this article.

References

- [1]. Feraboli P, Morris C, McLarty D., 2007. Design and certification of a composite thin-walled structure for energy absorption. *International Journal of Vehicle Design*, 44(3-4), pp.247-267.
- [2]. Seilsepour H, Zarastvand M, Talebitooti R., 2023. Acoustic insulation characteristics of sandwich composite shell systems with double curvature: The effect of nature of viscoelastic core. *Journal of Vibration and Control*, 29(5-6), pp.1076-1090.
- [3]. Zarastvand, Asadijafari, M., & Talebitooti, R., 2022. Acoustic wave transmission characteristics of stiffened composite shell systems with double curvature. *Composite Structures*, 292, p.115688.
- [4]. Talebitooti, R., & Zarastvand., 2018. The effect of nature of porous material on diffuse field acoustic transmission of the sandwich aerospace composite doubly curved shell. *Aerospace Science and Technology*, 78, pp.157-170.
- [5]. Talebitooti, R., Gohari, H., & Zarastvand., 2017. Multi objective optimization of

- sound transmission across laminated composite cylindrical shell lined with porous core investigating Non-dominated Sorting Genetic Algorithm. *Aerospace Science and Technology*, 69, pp.269–280.
- [6]. Boria S, Obradovic J, Belingardi G., 2015. Experimental and numerical investigations of the impact behavior of composite frontal crash structures. *Composite Part B Eng.*, 79, pp.20-27.
- [7]. Guades E, Aravinthan T, Islam M, Manalo A., 2012. A review on the driving performance of FRP composite piles. *Composite Structures*, 94(6), pp.1932-1942.
- [8]. Will MA, Franz T, Nurick GN., 2002. The effect of laminate stacking sequence of CFRP filament wound tubes subjected to projectile impact. *Composite Structures*, 58(2), pp.259-270.
- [9]. Lu G, Yu T., 2003. Energy Absorption of Structures and Materials. *Journal of composite Material*, 47, pp.22-42.
- [10]. Arnaud P, Hamelin P., 1998. Dynamic characterization of structures: a study of energy absorption in composite tubes. *Composite Science Technology*, 58(5), pp.709-715.
- [11]. Othman A, Abdullah S, Ariffin AK, Mohamed NAN., 2014. Investigating the quasi-static axial crushing behavior of polymeric foam-filled composite pultrusion square tubes. *Material Design*, 63, pp.446-459.
- [12]. Wang Y, Feng J, Wu J, Hu D., 2016. Effects of fiber orientation and wall thickness on energy absorption characteristics of carbon-reinforced composite tubes under different loading conditions. *Composite Structures*, 153, pp.356-368.
- [13]. Zhang X, Wen Z, Zhang H., 2014. Axial crushing and optimal design of square tubes with graded thickness. *Thin-Walled Structures*, 84, pp.263-274.
- [14]. Thornton PH, Harwood JJ, Beardmore P., 1985. Fiber-reinforced plastic composites for energy absorption purposes. *Compos Science Technology*, 24(4), pp.275-298.
- [15]. Farley GL, Jones RM., 1992. Crushing Characteristics of Composite Tubes with "Near-Elliptical" Cross Sections. *Journal of Composite Material*, 26(12), pp.1741-1751.
- [16]. Patel S, Vusa VR, Guedes Soares C., 2019. Crashworthiness analysis of polymer composites under axial and oblique impact loading. *International Journal of Mechanical Sciences*, 156, pp. 221-234.
- [17]. Song HW, Wan ZM, Xie ZM, Du XW., 2000. Axial impact behavior and energy absorption efficiency of composite wrapped metal tubes. *International Journal of Impact Engineering*, 24(4), pp.385-401.
- [18]. Kazemi ME, Kouchakzadeh MA, Shakouri M., 2020. Stability analysis of generally laminated conical shells with variable thickness under axial compression. *Mechanics of Advanced Materials and Structures*, 27(16), pp.1373-1386.
- [19]. Turner TA, Warrior NA, Robitaille F, Rudd CD., 2005. The influence of processing variables on the energy absorption of composite tubes. *Composite Part A Appl Sci Manuf.* 36(9), pp.1291-1299.
- [20]. Abosbaia AAS, Mahdi E, Hamouda AMS, Sahari BB., 2003. Quasi-static axial crushing of segmented and non-segmented composite tubes. *Composite Structures*. 60(3), pp.327-343.
- [21]. Melo JDD, Silva ALS, Villena JEN., 2008. The effect of processing conditions on the energy absorption capability of composite tubes. *Composite Structures*, 82(4), pp.622-628.
- [22]. Yan L, Chouw N., 2013. Crashworthiness characteristics of flax fiber reinforced epoxy tubes for energy absorption application. *Material Design*, 51, pp.629-640.
- [23]. Gupta NK, Easwara Prasad GL., 1999. Quasi-static and dynamic axial compression of glass/polyester composite hemi-spherical shells. *International Journal of Impact Engineering*, 22(8), pp.757-774.
- [24]. Karbhari VM, Haller JE, Falzon PK, Herszberg I., 1999. Post-impact crush of hybrid braided composite tubes. *International Journal of Impact Engineering*, 22(4), pp.419-433.
- [25]. Tong Y, Xu Y., 2018. Improvement of crash energy absorption of 2D braided composite tubes through an innovative chamfer external trigger. *International Journal of Impact Engineering*, 111, pp.11-20.
- [26]. Farley GL, Jones RM., 1992. Crushing Characteristics of Continuous Fiber-

- Reinforced Composite Tubes. *Journal of Composite Material*, 26(1), pp.37-50
- [27]. Palanivelu S, Van Paepegem W, Degrieck J, et al., 2010. Experimental study on the axial crushing behavior of pultruded composite tubes. *Polymer Testing*, 29(2), pp.224-234.
- [28]. Mahdi E, Hamouda AMS, Sebaey TA., 2014. The effect of fiber orientation on the energy absorption capability of axially crushed composite tubes. *Material Design*, 56, pp.923-928.
- [29]. Liu, X., Belkassam, B., Jonet, A., Lecompte, D., Van Hemelrijck, D., Pintelon, R., & Pyl, L., 2019. Experimental investigation of energy absorption behavior of circular carbon/epoxy composite tubes under quasi-static and dynamic crush loading. *Composite Structures*, 227(7), p.111266.
- [30]. Diniz, C. A., Pereira, J. L. J., Bortoluzzi, D. B., Cunha Jr, S. S., & Gomes, G. F., 2023. The influence of the type of fabric on the static and dynamic behavior of composite tubes with ply drop-off. *Engineering Structures*, 290(5), p.116380.
- [31]. Khan, R. A., & Mahdi, E., 2023. Effect of trigger mechanisms on the quasi-static axial crushing behavior of glass epoxy/polyvinyl chloride hybrid composite tubes. *Thin-Walled Structures*, 182(10), p.110306.
- [32]. Chen, D., Liu, Y., Meng, M., Li, B., Sun, X., Yang, B., Xiao, S., & Wang, T., 2023. Dynamic axial crushing behaviors of circular composite tubes with different reinforcing fibers and triggers. *International Journal of Mechanical Sciences*, 244(12), p.108083.